A DFT study of the electronic property of gold nanoclusters (Au$_x$, x = 1-12 atoms)

M.Sankaran and B.Viswanathan
Department of Chemistry,
Indian Institute of Technology, Madras
Chennai 600 036, INDIA

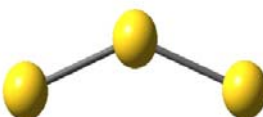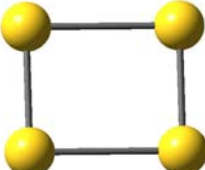**Abstract:** This communication attempts to find why Au$_8$ is more active as compared to other Au clusters.

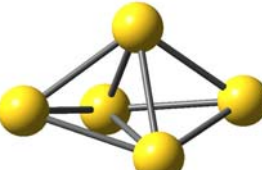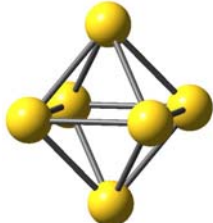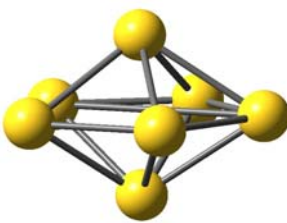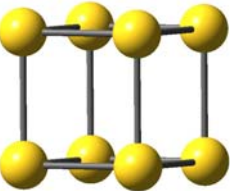Metallic nano particles especially that of gold and silver have received considerable attention in the past few years. Gold in the normal state is one of the inert materials with an ionization potential of 9.2 eV. For this reason, catalysis by gold has received limited attention in the past. However, supported nanosized gold particles have shown remarkable catalytic properties even for the oxidation of CO [1-3]. In addition, there appears to be a potential for exploitation of gold nano particles for a variety of applications including environmental pollution abatement, sensors and various other chemical and biochemical applications [4]. However, it is not yet clear why in the nano state or more appropriately in the suppor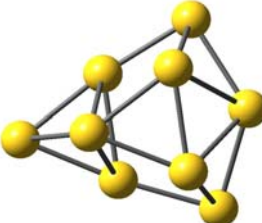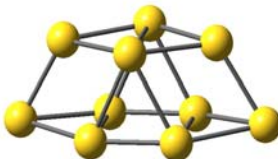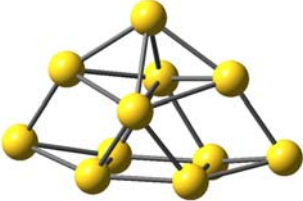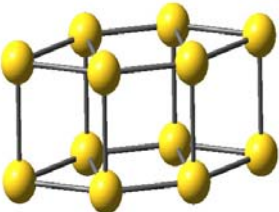ted state (supported on various oxides) gold shows remarkable activity for a variety of reactions and sensing applications. Sanchez et al., [5] have examined this question in detail and concluded that the partial electron transfer from the surface to the gold cluster and oxygen vacancy (F-center) defects play an essential role in the activation of nanosize gold clusters as catalysts and this result was further confirmed by recent investigation by Yoon et al., [6]. Recently, Gronbeck and Broqvist [7] have carried out a density functional calculations on Au$_8$ and have shown that the cluster prefers a two dimensional configuration while other metallic clusters like Cu$_8$ has a three dimensional structure. They have identified that d-electron delocalization as the cause for the two dimensional structure of gold clusters. Against this back ground, it has been attempted to examine a few other features of gold clusters with a view to understand the differences between various clusters Au$_x$ (where x = 1-12).

In the present investigation all the Density Functional Theory (DFT) calculations were carried out using Gaussian 03 program [8] in cluster of IBM Linux machine. The DFT calculations were carried out using Becke three parameter hybrids functional with Lee-Yan-Parr correlation function (B3LYP) [9] and an effective core potential basis set LANL2DZ (Los Alamos set of double-zeta) [10-13]. The DFT calculations using the LANL2DZ pseudopotentials is an adequate descriptor of Au cluster chemistry, which also includes the relativistic effect. Full geometry optimization and bond population analysis have been carried out for each cluster. Some of the earlier studies conducted on gold clusters using high level *ab initio* techniques were restricted to fixed symmetries and so excluded the possibility of disordered structures [14]. No symmetry constraints have been used

Table 1. The geometrical parameters of various gold clusters Au_x (where x= 2-12) optimized by DFT utilizing B3LYP/ LANL2DZ basis set.

Au$_2$ ***Au -Au bond length (Å)** 2.573 **Symmetric point group** $D_{\infty h}$	**Au$_3$** 2.640 C_{2V}	**Au$_4$** 3.118 / 2.576 D_{4h}	**Au$_5$** 2.807 / 2.754 C_{2V}
Au$_6$ 3.408 / 2.786 D_{4h}	**Au$_7$** 2.896 / 2.842 C_1	**Au$_8$** 2.767 C_1	**Au$_9$** 2.856 / 2.782 C_1
Au$_{10}$ 2.836 / 2.719 C_1	**Au$_{11}$** 2.773 / 2.849 C_1	**Au$_{12}$** 2.854 / 2.730 C_1	

*Where longest/ shortest Au-Au average bond length.

to the model and full optimization of the geometry is allowed. The optimized structure, average bond length and the symmetric point group of the clusters are given in Table 1. The Au_2 dimer is optimized to have bond length of 2.57Å with a symmetric point group of $D_{\infty h}$. Au_3 trimer forms bend structure compared to linear structure with an average Au-Au bond distance of 2.64 Å and bond angle of 140.7° having a planar geometry which appears more stable than a equilateral triangle with a side of 2.69 Å [15]. The formation of bend structure agrees with the earlier results that the gold monoatomic wires are zigzag shaped with a bond distance of 2.32 Å and a bond angle of 131° instead of linear structure. Unusual bond length is observed for the short gold nanowires [16, 17]. Au_4 cluster forms stable planar structure and rectangular shape with Au-Au bond distance of 2.58 and 3.12 Å, where as earlier reports show a distorted rhombus with D_{2h} symmetry. Au_5 forms a stable structure with C_{2V} symmetry which is more stable than the other structure. Au_6 optimizes at the most stable structure with D_{4h} symmetry with Au-Au bond distances of 3.41 Å and 2.79 Å forming an octahedral shape. The top and bottom Au atoms show a shorter bond length compared to others. Au_7 forms a stable pentagonal bipyramidal structure and Au_8 shows cubic structure and other clusters of 9 -12 atoms of Au shows a complex irregularity in three dimensional structure. The calculated electronic structure shows a transition from planar to non-planar geometry at n = 7 with C_1 symmetry. Comparing with experiment, transition to non-planar cluster geometries has been determined to take place at n = 7 on the basis of ion mobility measurement for Au cluster

cations [18]. The total energy and the stabilization energy of the clusters are given in Table 2. The stabilization energy values show a trend of increased stability with increase in the cluster size.
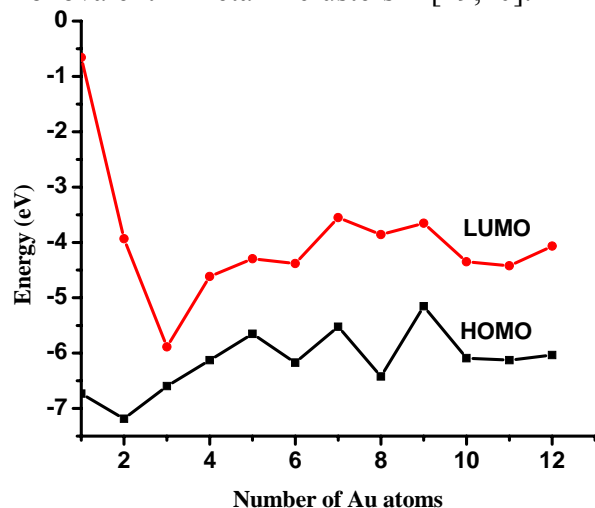
Table 2. The total energy and the stabilization energy of various gold clusters Au_x (where x= 1-12) optimized by DFT utilizing B3LYP / LANL2DZ basis set.

Cluster	Total energy (eV)	Stabilization energy* (eV)
Au	-3685.32	-
Au_2	-7372.50	-0.93
Au_3	-11058.70	-0.92
Au_4	-14745.19	-0.98
Au_5	-18432.03	-1.09
Au_6	-22119.02	-1.19
Au_7	-25806.59	-1.34
Au_8	-29493.40	-1.36
Au_9	-33180.88	-1.45
Au_{10}	-36868.19	-1.50
Au_{11}	-40555.20	-1.52
Au_{12}	-44241.83	-1.50

* Stabilization energy = [total energy of the cluster] – [No. of atoms] [energy of atom] / [total No. of atoms]

The frontier orbitals of the clusters were analyzed to find the highest occupied molecular orbitals (HOMO) and the lowest unoccupied molecular orbitals (LUMO) to get the energy difference between them. When there is a growth of cluster from the atom to bulk there exhibits closure of HOMO-LUMO energy difference and also development of collective electronic excitations [17]. The important criteria for the chemical stability of the cluster

are determined by their larger the HOMO – LUMO energy differences. Unusual high values of HOMO-LUMO gap are found at n = 2 and n = 8 which is seen from Fig 1. These values are consistent with the well known fact that HOMO – LUMO energy difference values are particularly large for n = 2, 8, .., the closed electronic shell in small monovalent metal clusters [19,20].

Figure 1. HOMO – LUMO energy levels of various gold clusters Au_x (where x= 1-12)

From the results of the calculations (Table 3.) Au_8 cluster shows a larger HOMO – LUMO difference compared to all other clusters. This causes a lower electron affinity [21], which in turn leads to higher catalytic activity.

Table 3. The HOMO and LUMO values of various gold clusters Au_x (where x = 1-12) optimized by DFT utilizing B3LYP/ LANL2DZ basis set.

| Cluster	HOMO (eV)	LUMO (eV)
Au	-6.733	-0.656
Au_2	-7.186	-3.935
Au_3	-6.596	-5.890
Au_4	-6.127	-4.615
Au_5	-5.651	-4.296
Au_6	-6.182	-4.382
Au_7	-5.522	-3.549
Au_8	-6.422	-3.857
Au_9	-5.152	--3.654
Au_{10}	-6.091	-4.350
Au_{11}	-6.127	-4.422
Au_{12}	-6.035	-4.067

The HOMO level of the clusters was analyzed and the results are given in Table 4. It is seen that the contribution of the orbitals are mainly from the '*s*' orbitals of the metal atom, whereas in the case of Au_8 cluster, maximum contribution is from the '*d*' orbitals. Detailed analysis of '*s*' and '*d*' contribution for the clusters of Au_x (x = 1-12) shows (Fig 2) that Au_8 only shows the major contribution from the '*d*' orbitals which could account for high catalytic activity.

Table 4. The percentage orbital contribution of HOMO level of various gold clusters Au_x (where x= 1-12) optimized by DFT utilizing B3LYP/ LANL2DZ basis set.

Cluster	Percentage orbital contribution		
	s	p	d
Au	100	-	-
Au_2	83.14	0.75	16.10
Au_3	86.40	5.51	8.05
Au_4	81.26	1.96	16.78

|			
Au$_5$	81.78	3.59	14.64
Au$_6$	74.67	6.72	18.63
Au$_7$	78.12	4.34	17.45
Au$_8$	**54.52**	**5.00**	**40.48**
Au$_9$	77.28	10.01	12.72
Au$_{10}$	74.99	4.92	20.10
Au$_{11}$	73.15	8.09	18.76
Au$_{12}$	53.55	28.35	18.10

The contribution of 's' and 'd' orbitals of the metal atoms to the various clusters is shown in Fig. 2.
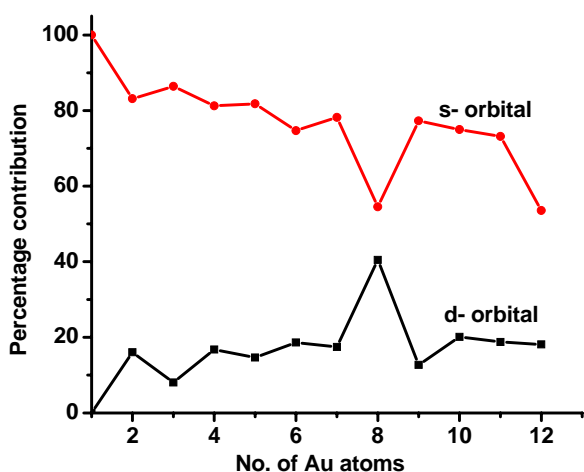
Figure 2. The percentage of s and d-orbital contributions of the various gold clusters Au$_x$ (where x= 1-12).

It is seen that only for the cluster Au$_8$, the HOMO level has predominant 'd' orbital contribution, where as for other clusters the HOMO level has maximum contribution from 's' orbital of the metal atoms. It is surprising that the 'd' orbital contribution to HOMO is increased to nearly 40% while the 's' orbital contribution is reduced to 55 for the Au$_8$ cluster atoms. In all other cluster (n ≤ 7 ≥ 9) the 's' orbital contribution is to HOMO level is nearly 70% or more. Fig 4. shows that the HOMO level is

spherically symmetrical for all clusters except Au$_8$. In the case of Au$_8$ cluster, the frontier orbital with nearly 40% 'd' character, is thus capable of overlapping with the frontier orbitals of the substrate molecules and hence accounts for the reactivity of Au$_8$ cluster. The (HOMO-LUMO) value which is a measure of the electron affinity of the system is also high for Au$_8$ cluster thus showing the higher reactivity to be expected.
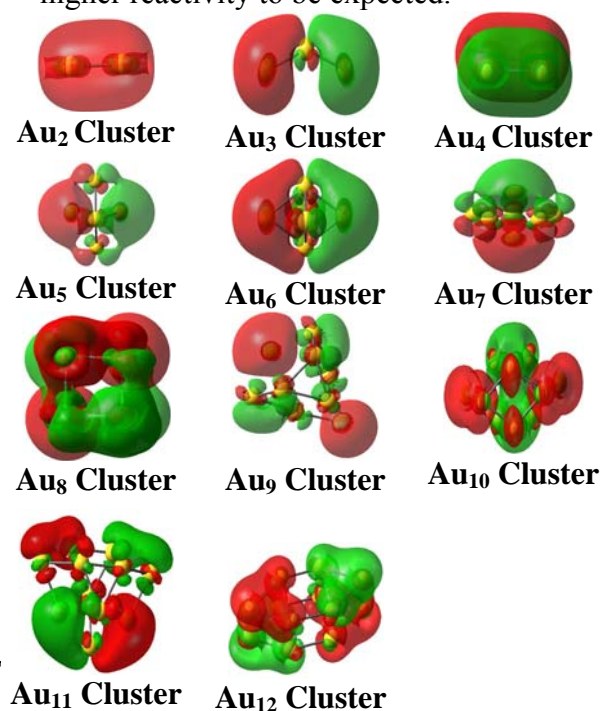
Figure 3. HOMO level frontier orbital contour of various gold clusters Au$_x$ (where x = 1-12). An isosurface value of 0.02 e/Å^3 was used for orbital. For the density plots, red indicates that the wave function has a negative sign, while green indicates a positive sign.

In summary, it is tempting to postulate the following. In the case of gold, a particular sized nanoparticles posses spatially oriented, symmetry allowed orbitals and the corresponding eigen values are appropriate for interaction with the incoming adsorbate molecules that undergo surface

transformations. For other sized nanoparticles the frontier wave functions have predominant '*s*' character and hence there is no spatial orientation or Eigen values matching and hence these other nanoparticles are not reactive enough. Due to these spatially oriented Eigen functions, these gold clusters interacted with support and the reactant system exhibits altered activity. It is proposed to probe further these postulates in a following communication.

References:
1. M. Haruta, Catal. Today 36 (1997) 153.
2. B.E. Solsona, M. Conte, Y. Cong, A.F. Carley, and G.J. Hutchings, Chem. Comm. (2005) 2351
3. S. Carrettin, P. Concepcion, A. Corma, J.M. Lopez Nieto and V.F. Puntes, Angew. Chem. Int. Ed. 43 (2004) 2538.
4. Special issue Edited by G.J. Hutchings and M. Haruta, Appl. Catal. A: Gen 291 (2005) 1.
5. H. Hakkinen, W. Abbet, A. Sanchez, U. Heiz and U. Landman, Angew. Chem. Int. Ed. 42 (2003) 1297.
6. B. Yoon, H. Hakkinen, U. Landman, A.S Worz, J. M. Antonietti, S. Abbet, K. Judai, U. Heiz. Science 307 (2005) 403.
7. H. Grönbeck and P. Broqvist. Phys. Rev. B 71 (2005) 073408.
8. M.J. Frisch, G.W. Trucks, H.B. Schlegel, G.E. Scuseria, M.A. Robb, J.R. Cheeseman, J.A. Montgomery Jr., T. Vreven, K.N. Kudin, J.C. Burant, J.M. Millam, S.S. Iyengar, J. Tomasi, V. Barone, B. Mennucci, M. Cossi, G. Scalmani, N. Rega, G.A. Petersson, H. Nakatsuji, M. Hada, M. Ehara, K. Toyota, R. Fukuda, J. Hasegawa, M. Ishida, T. Nakajima, Y. Honda, O. Kitao, H. Nakai, M. Klene, X. Li, J.E. Knox, H.P. Hratchian, J.B. Cross, C. Adamo, J. Jaramillo, R. Gomperts, R.E. Stratmann, O. Yazyev, A.J. Austin, R. Cammi, C. Pomelli, J.W. Ochterski, P.Y. Ayala, K. Morokuma, G.A. Voth, P. Salvador, J.J. Dannenberg, V.G. Zakrzewski, S. Dapprich, A.D. Daniels, M.C. Strain, O. Farkas, D.K. Malick, A.D. Rabuck, K. Raghavachari, J.B. Foresman, J.V. Ortiz, Q. Cui, A.G. Baboul, S. Clifford, J. Cioslowski, B.B. Stefanov, G. Liu, A. Liashenko, P. Piskorz, I. Komaromi, R.L. Martin, D.J. Fox, T. Keith, M.A. Al-Laham, C.Y. Peng, A. Nanayakkara, M. Challacombe, P.M.W. Gill, B. Johnson, W. Chen, M.W. Wong, C. Gonzalez and J.A. Pople, Gaussian 03, Revision C.02, Gaussian, Inc.; Wallingford, CT, 2004.
9. A.D. Becke, J. Chem. Phys. 98 (1993) 5648.
10. C. Lee, W. Yang and R.G. Parr, Phys. Rev. B 37 (1988) 785.
11. P.J. Hay and W.R Wadt , J. Chem. Phys 82 (1985) 270.
12. W.R Wadt and P.J. Hay, J. Chem. Phys 82 (1985) 284.
13. P.J. Hay and W.R. Wadt, J. Chem. Phys 82 (1985) 299.
14. O.D. Häberlan, S.-C. Chung, M. Stener and N. Rösch, J. Chem. Phys. 106 (1997) 5189.
15. D. Sa Anchez-Portal, J. Junquera, P. OrdejoAn, A. GarcoAa, E. Artacho, J. M. Soler, Stiff

Monatomic, Phys. Rev. Lett. 83 (1999) 3884.

16. J. Wang, G. Wang and Zhao, J. Phys. Rev. B 66 (2002) 035418.
17. N. Nilius, T. M. Wallis, W. Ho, Science 297 (2002)1853.
18. S. Gibbs, P. Weiss, F. Furche, R. Ahlrichs, M.M. Kappes, J. Chem. Phys. 116 (2002) 4094.
19. W.A. de Heer, Rev. Mod. Phys. 65 (1993) 611.
20. P. K. Jain, Structural Chemistry 16 (2005) 421.
21. N.S. Phala, G. klatt, E. van Steen, Chem. Phys. Lett, 395 (2004) 33.